Polymer Chemistry

Accepted Manuscript

This article can be cited before page numbers have been issued, to do this please use: A. K. Blakney, R. Liu, G. Yilmaz, Y. Abdouni, P. F. McKay, C. R. Bouton, R. J. Shattock and C. R. Becer, *Polym. Chem.*, 2020, DOI: 10.1039/D0PY00449A.

View Article Online
DOI: 10.1039/D0PY00449A

ARTICLE

Precisely Targeted Gene Delivery in Human Skin Using Supramolecular Cationic Glycopolymers

Received 00th January 20xx,
Accepted 00th January 20xx

DOI: 10.1039/x0xx00000x

Anna K. Blakney,[a†] Renjie Liu,[bc†] Gokhan Yilmaz,[d,e] Yamin Abdouni,[b] Paul F. McKay,[a] Clément R. Bouton,[a] Robin J. Shattock[a*] and C. Remzi Becer[b,e*]

Gene delivery has become the focus of clinical treatments, thus motivating delivery strategies that are capable of targeting certain cell types in the context of both vaccines and therapeutics. Here, we present a gene delivery platform enabled by host-guest interaction between a cyclodextrin with emanating chains of cationic polymers, poly (2-dimethylaminoethyl meth-acrylate) (PDMAEMA) paired with a glycosylated adamantane containing copolymer. By decoupling the cationic polymer and glycosylation chemistries, we were able to vary each independently to study the transfection efficiency both in vitro and ex vivo in human skin explants. Medium length PDMAEMA enabled optimal DNA complexation, and glycosylation specifically enhanced the number of cells transfected 100-fold in vitro and 3-fold ex vivo. Furthermore, these glycopoly-mers enabled greater immune cell up take, specifically in skin resident leukocytes. This platform is a facile and clinically translatable way to study how glycosylation affects cellular uptake and targeting in a complex cellular medium.

Introduction

Gene delivery is finally being realized in clinical products after years of academic research, thus motivating next-generation delivery platforms for vaccine and therapeutics.[1-2] Plasmid DNA (pDNA) has been effectively delivered with electroporation,[3] liposomes,[4] polyplexes[5-6] and emulsions.[7] However, these delivery vehicles do not intentionally target specific cellular subsets, which is known to be advantageous in both the context of therapeutics, such as hepatocytes for protein replacement,[8] and vaccines, i.e dendritic cells.[9] As intradermal injection is an advantageous route of administration for both thera-peutics[10] and vaccines,[11] we sought to develop a platform that would allow for targeted cellular uptake and gene delivery in human skin.

In the field of gene delivery, cationic polymers have been well-researched and proven to be efficient carriers for DNA and RNA molecules of various sizes.[12-14] Poly(ethylenimine) (PEI)[15] and poly (2-dimethylaminoethyl methacrylate) (PDMAEMA)[16] are the two most widely applied polymers for gene delivery purposes. Due to recent advancements in synthetic polymer chemistry, it is now possible to produce polymers with sophisticated architecture, such as multiblock copolymers and star-shaped polymers.[17-21] Star-shaped polymers have drawn increasing attention due to their unique behavior compared to their linear counterparts. Xue et al. reported the usage of star-shaped polymers as a platform for drug and gene co-delivery with better biocompatibility and responsive payload release profiles.[22] In addition, polymers with side carbohydrate units, glycopolymers, have been reported to interact with specific lectins due to the multivalent presentation of sugar molecules[23-25] and to improve the biocompatibility of synthetic polymers.[26] However, previously glycosylated cationic polymers are limited in tailoring of the amount of cationic charges pre-sent and degree of glycosylation when co-localized on a single molecular chain.[27-28] Thus, we sought a modular system in which we could decouple and individually tailor the cationic and glycosylated polymers to study cellular targeting of gene delivery complexes.

Host-guest chemistry through the interaction between cyclodextrin (CD) and adamantane (Ad) is a facile way to achieve advanced architectures such as single chain folding[29] and PEGylation of cationic polymers to improve circulation half-life.[30] Furthermore, CD and Ad have been shown to form specific and stable interactions in aqueous solution through the interaction between adamantane and the hydrophobic cavity of CD.[31-33] Thus this interaction has been widely utilized to form different functional materials, such as self-healing hydrogels[34-35] and drug carriers.[36-37] Due to the easily modifiable nature and biocompatibility of CD and Ad, we chose this host-guest pair as a platform to develop a glycosylated cationic polymer for gene delivery.

[a] Department of Medicine, Division of Infectious Diseases, Section of Immunology of infection, Imperial College London, Norfolk Place, London W21PG, UK.
[b] School of Engineering and Materials Science, Queen Mary University of London, London, E1 4NS, UK.
[c] J. Crayton Pruitt Family Department of Biomedical Engineering, Wertheim College of Engineering, University of Florida, Gainesville, FL 32611, USA.
[d] School of Pharmacy, University of Nottingham, Nottingham, NG7 2RD, UK.
[e] Department of Chemistry, University of Warwick, Coventry, CV4 7AL, UK.
† denotes equal contribution.
Electronic Supplementary Information (ESI) available: [details of any supplementary information available should be included here]. See DOI: 10.1039/x0xx00000x

View Article Online
DOI: 10.1039/D0PY00449A

Here, we present a gene delivery platform enabled by host-guest interaction of a star-shaped cationic PDMAEMA

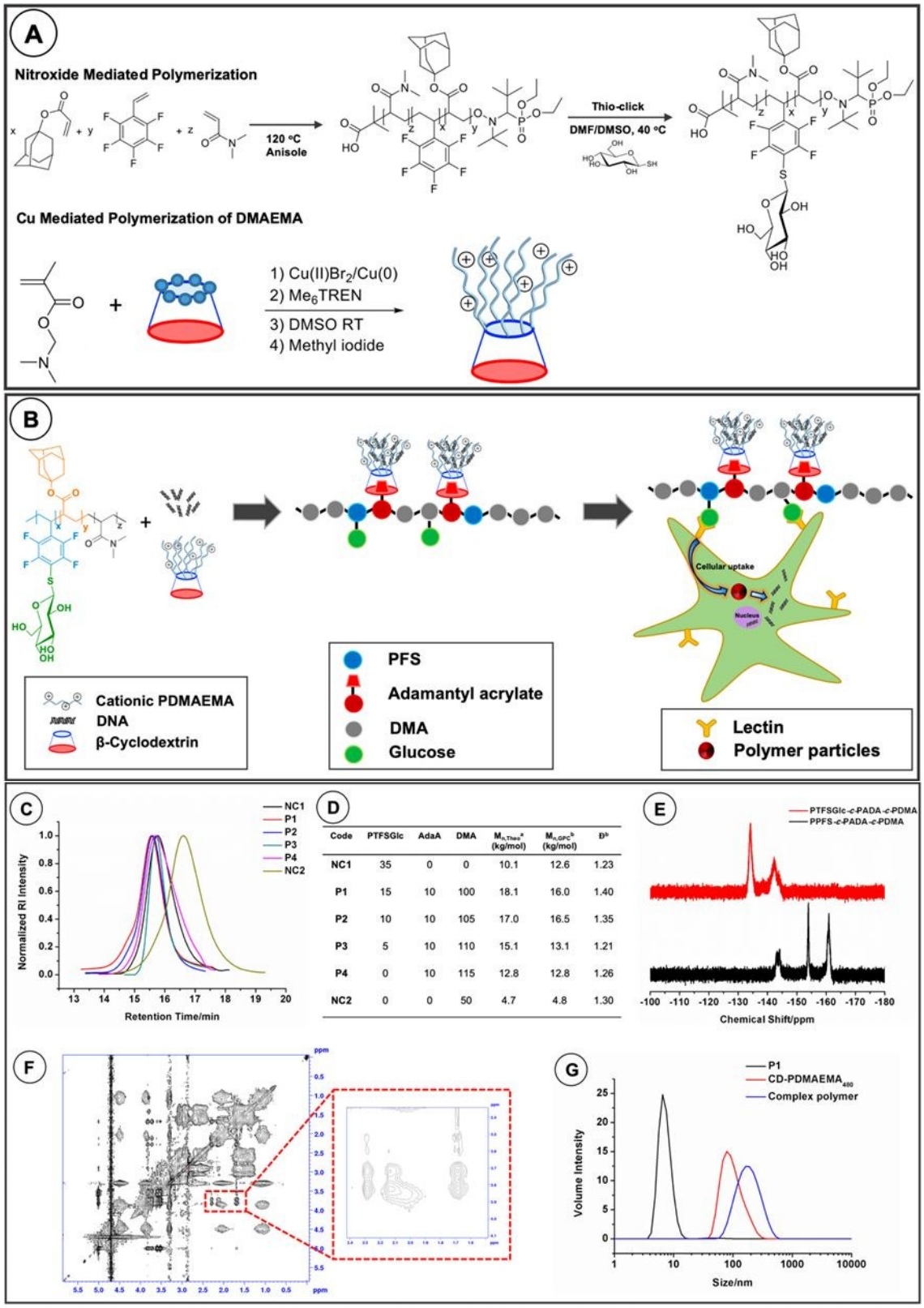

Figure 1. Polymerization scheme of the glycopolymer (**A**, **top**) and P(DMAEMA) complexation groups on the adamantane (**A**, **bottom**), schematic presentation of the complexation strategy (**B**), SEC traces of the obtained glycopolymers (**C**), the list of glycopolymers used in this study (**D**), ^{19}F NMR of the polymer to form a glycopolymer (**P1**) via para-fluoro-thiol click reaction (**E**),

View Article Online
DOI: 10.1039/D0PY00449A

2D NOESY NMR to demonstrate the complexation between CD and adamantane containing glycopolymer (**P1**) (**F**). DLS measurement demonstrated the complexation and size difference before and after complexation (**G**).

emanating from CD and an adamantane containing glycopolymer. We designed and synthesized a library of polymers with various molecular weights of PDMAEMA and degree of glycosylation. We then characterized the polymers, and the polyplexes formed when loaded with DNA for size, charge and transfection efficiency in vitro. After identifying the optimal PDMAEMA molecular weight for DNA loading, we tested the polyplexes ex vivo in human skin explants to characterize the transfection efficiency. Finally, we identify the phenotypes of transfected cells and determine the specifically targeting among all cell populations.

Results and Discussion

Glycopolymer synthesis and characterization

Adamantane containing terpolymers with a various number of carbohydrates and CD-initiated cationic PDMAEMA were designed and synthesized, as shown in **Figure 1A** and **1B**. Through the host-guest chemistry between adamantane and CD, the obtained nanostructured complexes allow for further electrostatic interactions with negatively charged DNA molecules to obtain a useful platform for DNA delivery. Glycan moieties on the complexes are suitable for cellular targeting by engaging with lectins on the cell surface, as previously reported.[24, 38-41]

PTFSGlc-r-PAdaA-r-PDMA was firstly synthesized using nitroxide mediated polymerization (NMP) and followed by a para-fluorine substitution reaction with 1-thio-β-D-glucose (**Figure 1A**). NMP was chosen here to avoid left-over containments such as metal species or sulfur-containing compound, which could complicate further biological experiments. Besides, it is applicable to different types of monomers to polymerize with a good control.[42] Copolymers with different monomer ratios were synthesized to elucidate the influence of carbohydrate density on cellular targeting and uptake. In the meantime, seven arm star-shaped PDMAEMA was prepared using CD initiator in DMSO at room temperature by Single Electron Transfer-Living Radical Polymerization (SET-LRP) (**Figure 1A**). The star-shaped PDMAEMA was further reacted with methyl iodide (CH_3I) to introduce cationic charges on the polymers. Cationic PDMAEMA with different chain lengths was prepared in order to optimize the loading efficiency of DNA. **Figure 1C** shows the GPC traces of the copolymers and negative controls (PTFSGlc for **NC1** and PDMA for **NC2**). **Figure 1D** shows the molecular weight and polydispersity of the obtained polymers. All the copolymers have relatively similar hydrodynamic volume and narrow polydispersity values without significant tailing or coupling peaks. As seen in **Figure S4**, the ^1H NMR of t_0 and t_{final} reaction mixture were used here to calculate each monomer conversion and their relative ratios in the final copolymers. This method was chosen here due to the small amount of PFS and adamantane acrylate in the final co-polymers which make it impossible to directly calculate their relative ratio in the final copolymers (data not shown here). As depicted in **Figure S5**, the GPC traces of PDMAEMAs also indicated that PDMAEMA with 48, 68 and 80 repeating units on each arm possess an increased hydrodynamic volume with longer chain length. ^{19}F NMR was also measured here to characterize the efficiency of para-fluorine substitution reactions (**Figure 1E** and **Figure S6**). The spectrum shows the complete disappearance of para-fluorine which proves the full substitution of para-fluorine on PFS. In summary, tri-copolymers with different monomer ratios and PDMAEMAs with different chain length were successfully synthesized with precise control over polymer properties.

Glycopolymer/DNA particle characterization

After the preparation of copolymers and star-shaped polymers, the physical interaction between adamantane protons and β-cyclodextrin cavity was confirmed using 2D NOESY NMR (**Figure 1F**) to observe the formation of complexes in the aqueous phase. The interaction peaks from adamantane protons (1.6-2.3 ppm) and the inner protons from CD cavity (3.6-3.9 ppm) showed the direct interaction of protons on the host-guest molecules (**Figure 1F**). Dynamic light scattering (DLS) was also employed here to characterize the size evolution during the complex formation (**Figure 1G** and **Figure S7**). Results showed a single population of smaller particles before mixing and an increase of complex size after the complex formation. Both of these confirmed the specific and successful interaction between adamantane containing glycopolymers and cationic star-shaped polymers which leads to the formation of carbohydrate decorated cationic complexes with various sizes (**Figure S7**). Zeta-potential was also measured after the complex formation with DNA (**Figure 2B**). All the complexes remained cationic charged after mixing which shows the host-guest interaction does not interfere with the cationic charges on the polymer brushes which allow further condensation with anionic DNA molecules. Interestingly, decreases of complex sizes were observed after mixing with DNA (**Figure 2A**), which we hypothesize was caused by the neutralization of charges by DNA molecules and lowering of the repulsion between polymer brushes.

Glycopolymers enhance transfection efficiency in vitro

In order to investigate the effects of PDMAEMA length and glycosylation on transfection efficiency in vitro, we first prepared complexes with DNA and CD-PDMAEMA polymers with varying DMAEMA length and varying ratios of PDMAEMA to DNA (**Figure 2C**). We observed that increasing the DMAEMA length profoundly impacted the transfection efficiency; increasing the DMAEMA length from 336 repeat units to 480 units increased the transfection efficiency by ~3 orders of magnitude. We postulate that this phenomenon is due to steric hindrance between the cyclodextrin and PDMAEMA brushes that may exclude the pDNA. The two longer PDMAEMA brushes had equivalent transfection efficiency,

View Article Online
DOI: 10.1039/D0PY00449A

~106 RLU even at the lowest ratio of polymer to DNA tested (10:1, w/w (N/P=6-7)), and there was no added benefit to increasing the ratio. The CD-PDMAEMA-336 complexed exhibited a trend of increasing transfection efficiency with increasing ratio of polymer to DNA, however; at the highest ratio of 500:1 (w/w) (N/P=2988-3215) it was still ~2 orders of magnitude lower than the

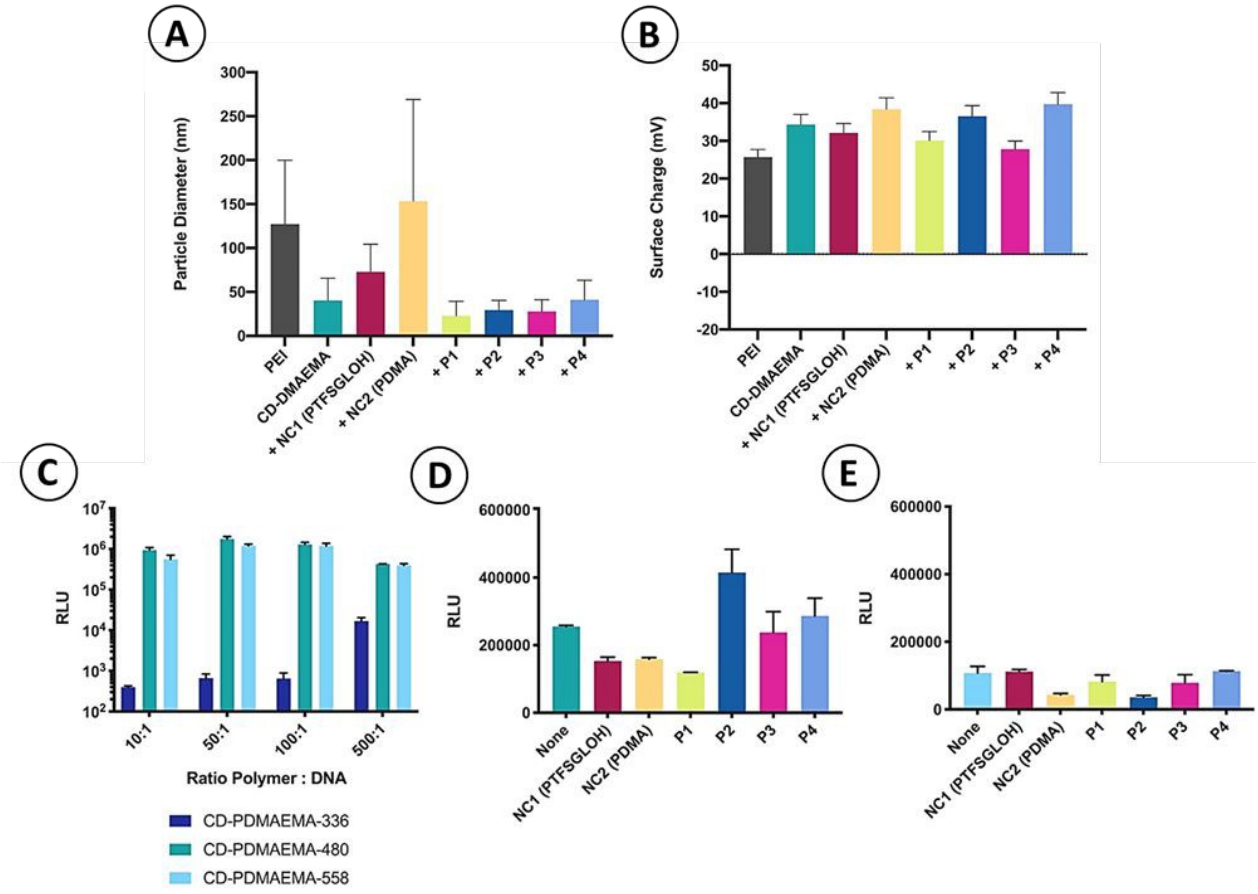

Figure 2. In vitro particle characterization and transfection efficiency of Luciferase-encoding pDNA complexed with PDMAEMA-CD-Ad-Glu polymers. **A**) Hydrodynamic diameter and **B**) zeta potential of PTFSGlc-c-PAdaA-c-PDMA, PDMAEMA and pDNA complex at a ratio of 10:1 polymer to pDNA (w/w) (N/P=6-7) using DLS. Bars represent mean ± standard deviation for n=3. **C-E**) Transfection efficiency of CD-PMAEMA polymers complexed with DNA in HEK 293T.17 cells with **C**) (no Ad-Glu) at varying ratios from 10:1 to 500:1, **D**) CD-PDMAEMA-480 and **E**) CD-PDMAEMA-558 complexed with **P1-4** at a ratio of 10:1 polymer to pDNA (w/w) (N/P=6-7). Bars represent mean ± standard deviation for n=3. RLU= relative light units. pDNA has 7047 base pairs.

CD-PDMAEMA-480 and CD-PDMAEMA-558 and thus this polymer was excluded from future studies. These results reflect previous reports that increasing PDMAEMA length can enhance the transfection efficiency in vitro.[43-44] Other than this, due to the significant differences in three monomer structures, control over monomer ratio could also lead to a morphological change of the final copolymers as reported before, which could influence the final DNA complexation process.[45,46] All of these could contribute the increase of DNA loading capacity with increased polymer chain length. We then sought to characterize how the host-guest inter-action between cyclodextrin and adamantane affected the transfection efficiency of CD-PDMAEMA polymers (**Figure 2D-E**). We utilized CD-PDMAEMA-480 and CD-PDMAEMA-558 complexed with the glycosylated adamantane polymers (**P1-P4**), as well as two negative controls (**NC1-NC2**). Complexation with the negative controls (PTFSGLOH and PDMA) decreased transfection efficiency for both CD-PDMAEMA-480 and CD-PDMAEMA-558. However, complexing CD-PDMAEMA-480 with **P2**, **P3** and **P4** slightly enhanced transfection efficiency (**Figure 2D**). Interestingly, we did not observe this effect for CD-PDMAEMA-558 (**Figure 2E**), which had similar transfection levels when complexed with **P1-P4**. We hypothesize that this is due to steric hindrance in the particles, wherein there may be an optimal PDMAEMA length that facilitates complexation with DNA but does not mask availability of glycan groups. Overall, we observed that increasing the PDMAEMA length increased transfection efficiency of CD-PDMAEMA/pDNA complexes, and that the complexation of glycosylated adamantane with medium length CD-PDMAEMA yielded glycan-specific enhanced transfection. Besides, these

polyplexes represented greater than 80% viability through human skin cells (**Figure S9**).

Glycosylation enhances cellular uptake in human skin explants

Given the promising transfection results, we sought to test the glycopolymers in a more clinically translational human skin explant model. Human skin explants have previously been shown as a viable way to evaluate nucleic acid formulations, and contain many cell types with lectin-binding domains.[47,48] Complexes of CD-PDMAEMA-480 alone or paired with **P1-4** or **NC1-2** were compared to eGFP-encoding DNA alone and PEI as

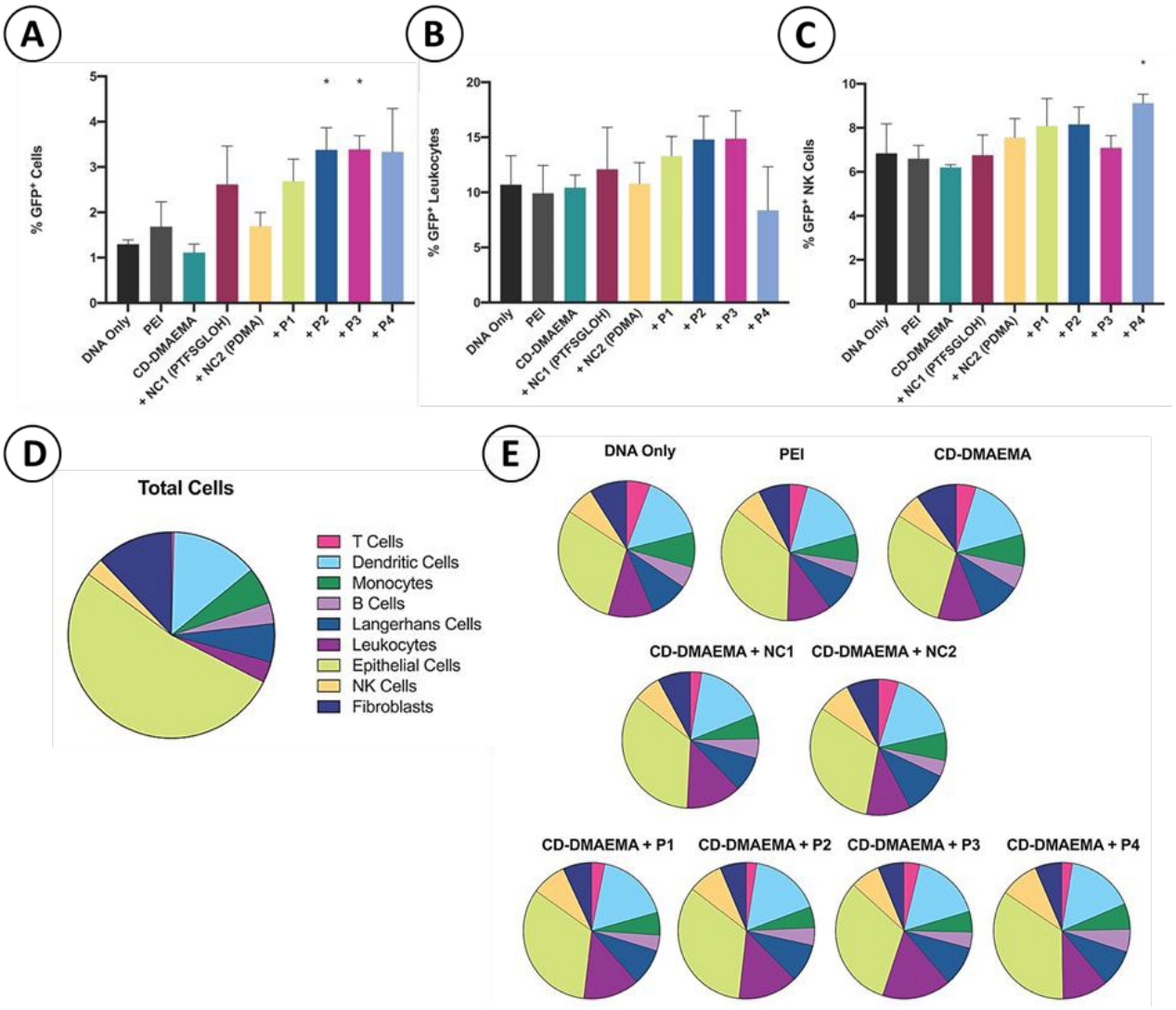

Figure 3. GFP expression in human skin cells after intradermal injection with DMAEMA-CD-Ad-Glu/pDNA polyplexes at a ratio of 10:1 polymer to pDNA (w/w) (N/P=6-7) as determined by flow cytometry. **A**) Percentage of GFP+ cells of total live cells for each sample, **B**) percentage of GFP+ leukocytes and **C**) NK cells. Bar represents average ± standard deviation, * represents significance compared to DNA alone, with $\alpha<0.05$. **D**) Identity of cells present in human skin explants and **E**) GFP+ cells after ID injection of DMAEMA-CD-Ad-Glu/pDNA polyplexes as determined by flow cytometry. Cells were identified using the following antibodies: epithelial cells (CD45-), fibroblasts (CD90+), NK cells (CD56+), leukocytes (CD45+), Langerhans cells (CD1a+), monocytes (CD14+), dendritic cells (CD11c+), T cells (CD3+) and B cells (CD19+). The used pDNA has 7047 base pairs.

a positive control (**Figure 3A** and **S8**). DNA alone resulted in only ~1% of cells expressing eGFP, and there was no increase when complexed to PEI or CD-DMAEMA alone. However, when paired with the adamantane polymers, **P1-P4**, there was a 3-fold increase in eGFP-expressing cells, although only glycosylated **P2** and **P3** were found to be statistically significant (p= 0.047 and 0.033, respectively). While there was no enhancement with **NC2**, there was slight increase in the percentage of eGFP expressing cells with **NC1**, which we hypothesize may be due to non-specific interaction between **NC1** and the CD-DMAEMA; however, it was not statistically significantly different than DNA alone. Thus, glycosylation of CD-PDMAEMA polymers increases the percentage of eGFP+ cells compared to DNA, PEI and CD-PDMAEMA alone. We then sought to determine whether the increased transfection efficiency was due simply to the quantity of cells expressing

eGFP, or whether there was more expression of eGFP on a per cell basis. This is observed by using a histogram plot of number of cells versus GFP intensity (**Figure S8**), wherein an in-crease in cells is shown on the y-axis and a shift in the GFP fluorescence on the x-axis indicates higher GFP expression per cell. The representative peaks for each group show that the increased protein expression is due to a higher number of cells expressing eGFP, as there is no shift in the median fluorescence intensity (MFI) for any of the samples. We postulate that this is because once the DNA reaches the nucleus, the eGFP translation is maximized. Thus, it is beneficial to use delivery vehicles such as these glycosylated CD-PDMAEMA polymers that are capable of targeting an increased number of cells in human skin explants for maximal transfection efficiency.

Phenotypic identity of cells expressing glycopolymer-delivered DNA in human skin explants

After observing that these glycopolymers enhanced the number of cells expressing eGFP in human skin explants, we then characterized which cells were expressing eGFP in order to determine if these polymers were targeting specific cell subsets (**Figure 3D-E**). We utilized a flow cytometry panel capable of identifying epithelial cells (CD45-), fibroblasts (CD90+), NK cells (CD56+), leukocytes (CD45+), Langerhans cells (CD1a+), monocytes (CD14+) dendritic cells (CD11c+), T cells (CD3+) and B cells (CD19+). We observed that the majority of the cells present in human skin explants were epithelial cells, fibroblasts and dendritic cells. While the DNA, PEI and CD-DMAEMA formulations were taken up primarily by epithelial cells (~30%), fibroblasts (~9%), and DCs (~15%), they were observed in all the evaluated cell types evaluated, including leukocytes (~11%), Langerhans cells (~9%), monocytes (~8%), NK cells (~7%), T cells (~6%), and B cells (~5%). CD-DMAEMA polymers had slightly varied phenotypic expression profiles when complexed with the glycosylated adamantane polymers, including a slight reduction in expression in monocytes (~5%), T cells (~4%) and B cells (~4%), and a trend of higher expression in leukocytes (~16%) and NK cells (~7%) (**Figure 3B-C**). CD-PDMAEMA complexed with **P2** and **P3** showed a slight increase in leukocyte eGFP expression, indicating that the middle amounts of glycosylation may be optimal for leukocyte targeting and reflecting the increased number of cells expressing eGFP in **Figure 3A** and **S8**. This mechanism may be similar to known leukocyte recognition of lectins, that enable cellular binding and uptake.[49-50] Interestingly, **P4** showed significantly higher expression in NK cells (p=0.023), despite no glycosylation. We suspect that this is due to the co-localization of multiple CD-PDMAEMA groups on a single polymer DMA chain which enables greater uptake in NK cells, and may be related to known NK cells recognition of haptens or virus like particles (VLPs).[51] Overall, glycosylation of CD-PDMAEMA polymers enabled higher expression in immune cells, and specifically leukocytes, compared to DNA alone, PEI and control polymers.

Conclusions

We designed a library of cationic polymers that are paired with glycopolymers through host-guest interactions for targeted gene delivery. We show that the medium length CD-PDMAEMA polymer is optimal for DNA complexation and in vitro transfection. Complexing the CD-PDMAEMA polymers with glycosylated adamantane polymers enhanced transfection both in vitro and ex vivo, which was specifically increased due to glycosylation. We demonstrated that the elevated protein expression ex vivo was due to an increased number of transfected cells as op-posed to the per cell expression, and that glycosylation showed a trend of increasing the number of leukocytes expressing GFP. We believe that this platform will be highly useful for exploring how different glycan groups affect cellular uptake and targeting in different tissues, and represent a clinically translational relevant approach for targeted gene delivery.

Conflicts of interest

There are no conflicts to declare.

Notes

All experiments were performed in accordance with the Guidelines of the Human Tissue Authority and were approved by the Local Research Ethics Committee at Imperial College London. Informed consents were obtained from human participants of this study. For the ex vivo studies surgically resected specimens of human skin tissue were collected at Charing Cross Hospital, Imperial NHS Trust, London, UK. All tissues were collected after receiving signed informed consent from patients, under protocols approved by the Local Research Ethics Committee (MED_RS_11_014) at Imperial College London. The tissue was obtained from patients undergoing elective abdominoplasty or mastectomy surgeries.

Acknowledgements

AKB is supported by a Whitaker Post-Doctoral Fellowship and a Marie Skłodowska Curie Individual Fellowship funded by the European Commission H2020 (No. 794059). PFM, CRB and RJS are funded by the U.K. Department of Health and Social Care for funding the Future Vaccine Manufacturing Hub through the Engineering and Physical Sciences Research Council (EPSRC, grant number: EP/R013764/1). GY was funded by EPSRC (EP/P009018/1) and RL was funded by the China Scholarship Council (CSC) and Queen Mary, University of London.

We gratefully acknowledge the surgeons at Charing Cross Hospital, Elizabeth A. Dex and Judith E. Hunter, and their nursing team for providing the tissue used in these experiments. We also acknowledge Dormeur Investment Services Ltd for providing funds to purchase equipment used in these studies.

References

1. N. Pardi, M. J. Hogan, F. W. Porter and D. Weissman, Nature reviews. Drug discovery, 2018, 17, 261-279.
2. L. Lambricht, A. Lopes, S. Kos, G. Sersa, V. Préat and G. Vandermeulen, Expert Opinion on Drug Delivery, 2016, 13, 295-310.
3. J. F. S. Mann, P. F. McKay, A. Fiserova, K. Klein, A. Cope, P. Rogers, J. Swales, M. S. Seaman, B. Combadiere and R. J. Shattock, Journal of Virology, 2014, 88, 6959.
4. P.-Y. Chien, J. Wang, D. Carbonaro, S. Lei, B. Miller, S. Sheikh, S. M. Ali, M. U. Ahmad and I. Ahmad, Cancer Gene Therapy, 2004, 12, 321.
5. S. Mao, W. Sun and T. Kissel, Advanced Drug Delivery Reviews, 2010, 62, 12-27.
6. J. F. S. Mann, P. F. McKay, S. Arokiasamy, R. K. Patel, K. Klein and R. J. Shattock, Journal of Controlled Release, 2013, 170, 452-459.
7. C.-H. Liu and S.-Y. Yu, Colloids and Surfaces B: Biointerfaces, 2010, 79, 509-515.
8. N. Mishra, N. P. Yadav, V. K. Rai, P. Sinha, K. S. Yadav, S. Jain and S. Arora, Biomed Res Int, 2013, 2013, 382184-382184.
9. C. Macri, C. Dumont, A. P. Johnston and J. D. Mintern, Clin Transl Immunology, 2016, 5, e66-e66.
10. S. Golombek, M. Pilz, H. Steinle, E. Kochba, Y. Levin, D. Lunter, C. Schlensak, H. P. Wendel and M. Avci-Adali, Molecular therapy. Nucleic acids, 2018, 11, 382-392.
11. P. H. Lambert and P. E. Laurent, Vaccine, 2008, 26, 3197-3208.
12. A. K. Blakney, G. Yilmaz, P. F. McKay, C. R. Becer and R. J. Shattock, Biomacromolecules, 2018, 19, 2870-2879.
13. S. C. De Smedt, J. Demeester and W. E. Hennink, Pharmaceutical research, 2000, 17, 113-126.
14. D. G. Anderson, D. M. Lynn and R. Langer, Angewandte Chemie International Edition, 2003, 42, 3153-3158.
15. W. Godbey, K. K. Wu and A. G. Mikos, Journal of controlled release, 1999, 60, 149-160.
16. S. Agarwal, Y. Zhang, S. Maji and A. Greiner, Materials Today, 2012, 15, 388-393.
17. F. Alsubaie, A. Anastasaki, P. Wilson and D. M. Haddleton, Polym. Chem., 2014, 6, 406-417.
18. R. Aksakal, M. Resmini and C. Becer, Polym. Chem., 2016, 7, 171-175.
19. R. Liu, D. Patel, H. R. Screen and C. R. Becer, Bioconjug Chem., 2017, 28, 1955-1964.
20. A. H. Soeriyadi, C. Boyer, F. Nyström, P. B. Zetterlund and M. R. Whittaker, Journal of the American Chemical Society, 2011, 133, 11128-11131.
21. R. Liu, C. R. Becer and H. R. Screen, Macromol. Biosci., 2018, 18, 1800293.
22. D. Ma, Q.-M. Lin, L.-M. Zhang, Y.-Y. Liang and W. Xue, Biomaterials, 2014, 35, 4357-4367.
23. C. Lavilla, G. Yilmaz, V. Uzunova, R. Napier, C. R. Becer and A. Heise, Biomacromolecules, 2017, 18, 1928-1936.
24. Q. Zhang, L. Su, J. Collins, G. Chen, R. Wallis, D. A. Mitchell, D. M. Haddleton and C. R. Becer, J. Am. Chem. Soc., 2014, 136, 4325-4332.
25. C. R. Becer, M. I. Gibson, J. Geng, R. Ilyas, R. Wallis, D. A. Mitchell and D. M. Haddleton, J. Am. Chem. Soc., 2010, 132, 15130-15132.
26. E. H. Wong, M. M. Khin, V. Ravikumar, Z. Si, S. A. Rice and M. B. Chan-Park, Biomacromolecules, 2016, 17, 1170-1178.
27. C. Boyer, N. A. Corrigan, K. Jung, D. Nguyen, T.-K. Nguyen, N. N. M. Adnan, S. Oliver, S. Shanmugam and J. Yeow, Chemical Reviews, 2016, 116, 1803-1949.
28. M. Hashida, M. Nishikawa, F. Yamashita and Y. Takakura, Advanced Drug Delivery Reviews, 2001, 52, 187-196.
29. G. Yilmaz, V. Uzunova, R. Napier and C. R. Becer, Biomacromolecules, 2018, 19, 3040-3047.
30. S. H. Pun, N. C. Bellocq, A. Liu, G. Jensen, T. Machemer, E. Quijano, T. Schluep, S. Wen, H. Engler, J. Heidel and M. E. Davis, Bioconjugate Chemistry, 2004, 15, 831-840.
31. M. Miyauchi and A. Harada, Journal of the American Chemical Society, 2004, 126, 11418-11419.
32. J. Wang and M. Jiang, Journal of the American Chemical Society, 2006, 128, 3703-3708.
33. G. Yilmaz, V. Uzunova, R. M. Napier and C. R. Becer, Biomacromolecules, 2018, 3040–3047.
34. T. Kakuta, Y. Takashima, M. Nakahata, M. Otsubo, H. Yamaguchi and A. Harada, Advanced materials, 2013, 25, 2849-2853.
35. K. Miyamae, M. Nakahata, Y. Takashima and A. Harada, Angewandte Chemie International Edition, 2015, 54, 8984-8987.
36. C. Y. Ang, S. Y. Tan, X. Wang, Q. Zhang, M. Khan, L. Bai, S. T. Selvan, X. Ma, L. Zhu and K. T. Nguyen, Journal of Materials Chemistry B, 2014, 2, 1879-1890.
37. Y. Shi, J. Goodisman and J. C. Dabrowiak, Inorganic chemistry, 2013, 52, 9418-9426.
38. A. Restuccia, M. M. Fettis, S. A. Farhadi, M. D. Molinaro, B. Kane and G. A. Hudalla, ACS Biomater. Sci. Eng., 2018, 4, 3451-3459.
39. Q. Zhang, J. Collins, A. Anastasaki, R. Wallis, D. A. Mitchell, C. R. Becer and D. M. Haddleton, Angew. Chem. Int. Ed., 2013, 52, 4435-4439.
40. M. Ahmed, R. Narain, Biomaterials, 2011**,** 32, 5279-5290.
41. M. Tranter, Y. Liu, S. He, J. Gulick, X. Ren, J. Robbins, W. K. Jones, T. M. Reineke, Molecular Theraphy, 2012**,** 20, 601-608.
42. S. Aksakal, R. Liu, R. Aksakal and C. R. Becer, Polym. Chem., 2020, 11, 982-989.
43. C. Arigita, N. J. Zuidam, D. J. A. Crommelin and W. E. Hennink, Pharmaceutical Research, 1999, 16, 1534-1541.
44. Y. Zhang, M. Zheng, T. Kissel and S. Agarwal, Biomacromolecules, 2012, 13, 313-322.
45. A. Blanazs, S. P. Armes and A. J. Ryan, Macromolecular rapid communications, 2009, 30, 267-277.
46. J. Zhu, Y. Jiang, H. Liang and W. Jiang, The Journal of Physical Chemistry B, 2005, 109, 8619-8625.
47. S. Ebner, Z. Ehammer, S. Holzmann, P. Schwingshackl, M. Forstner, P. Stoitzner, G. M. Huemer, P. Fritsch and N. Romani, International Immunology, 2004, 16, 877-887.
48. P. J. A. HOLT, J. HILLANGLIN JR and R. E. NORDQUIST, British Journal of Dermatology, 1979, 100, 237-245.
49. M. M. Fernández, F. Ferragut, V. M. Cárdenas Delgado, C. Bracalente, A. I. Bravo, A. J. Cagnoni, M. Nuñez, L. G. Morosi, H. R. Quinta, M. V. Espelt, M. F. Troncoso, C. Wolfenstein-Todel, K. V. Mariño, E. L. Malchiodi, G. A. Rabinovich and M. T. Elola, Biochimica et Biophysica Acta (BBA) - General Subjects, 2016, 1860, 2255-2268.
50. K. Ley, P. Gaehtgens, C. Fennie, M. S. Singer, L. A. Lasky and S. D. Rosen, Blood, 1991, 77, 2553.
51. E. Lugli, K. Hudspeth, A. Roberto and D. Mavilio, European Journal of Immunology, 2016, 46, 1809-1817.

View Article Online
DOI: 10.1039/D0PY00449A

Graphical of Abstract